

Additive Schwarz methods for the Crouzeix-Raviart mortar finite element for elliptic problems with discontinuous coefficients

Talal Rahman, Xuejun Xu, Ronald H. W. Hoppe

Angaben zur Veröffentlichung / Publication details:

Rahman, Talal, Xuejun Xu, and Ronald H. W. Hoppe. 2005. "Additive Schwarz methods for the Crouzeix-Raviart mortar finite element for elliptic problems with discontinuous coefficients." *Numerische Mathematik* 101 (3): 551–72.
<https://doi.org/10.1007/s00211-005-0625-2>.

Nutzungsbedingungen / Terms of use:

licgercopyright

Dieses Dokument wird unter folgenden Bedingungen zur Verfügung gestellt: / This document is made available under the following conditions:

Deutsches Urheberrecht

Weitere Informationen finden Sie unter: / For more information see:

<https://www.uni-augsburg.de/de/organisation/bibliothek/publizieren-zitieren-archivieren/publizieren>



Talal Rahman · Xuejun Xu · Ronald Hoppe

Additive Schwarz methods for the Crouzeix-Raviart mortar finite element for elliptic problems with discontinuous coefficients

Abstract In this paper, we propose two variants of the additive Schwarz method for the approximation of second order elliptic boundary value problems with discontinuous coefficients, on nonmatching grids using the lowest order Crouzeix-Raviart element for the discretization in each subdomain. The overall discretization is based on the mortar technique for coupling nonmatching grids. The convergence behavior of the proposed methods is similar to that of their closely related methods for conforming elements. The condition number bound for the preconditioned systems is independent of the jumps of the coefficient, and depend linearly on the ratio between the subdomain size and the mesh size. The performance of the methods is illustrated by some numerical results.

Mathematics Subject Classification (2000) 65F10 · 65N30

This work has been supported in part by the Bergen Center for Computational Science, University of Bergen.

This work has been supported by the Alexander von Humboldt Foundation and the special funds for major state basic research projects (973) under 2005CB321701 and the National Science Foundation (NSF) of China (No.10471144).

T. Rahman (✉)

Bergen Center for Computational Science, University of Bergen, Thormøhlensgt. 55,
5008 Bergen, Norway
E-mail: talal@bccs.uib.no

X. Xu

LSEC, Institute of Computational Mathematics, Chinese Academy of Sciences, P.O.Box 2719,
Beijing, 100080, People's Republic of China
E-mail: xxj@lsec.cc.ac.cn

R. Hoppe

Department of Mathematics, University of Houston, Calhoun Street, Houston, TX77204-3008,
USA
and Institute of Mathematics, University of Augsburg, Universitätsstr. 14, 86159 Augsburg,
Germany
E-mail: hoppe@math.uni-augsburg.de; rohop@math.uh.edu

1 Introduction

We consider the numerical solution of second order elliptic problems with discontinuous coefficients. Such problems play an important role in scientific computation, for instance, in the simulation of fluid flow in porous media, where the permeability of the porous media may have discontinuities across interior boundaries (or subdomain interfaces). It is well known that these discontinuities or jumps in the coefficients cause difficulties for standard iterative schemes, the performance of these methods deteriorates as the jumps increase. Over the past years, several numerical techniques dealing with jump coefficients have been developed, including techniques based on adaptive refinement [7,35,36], domain decomposition [8–11,21–24,31,39], and interface relaxation [41].

Mortar techniques on nonmatching meshes have recently attracted a lot of attention, since they provide a more flexible approach than standard discretization techniques, for instance, in handling problems with complicated geometries and heterogeneous materials, in developing parallel algorithms for the discretization, etc. The general concept for mortar techniques was originally introduced by Bernardi, Maday and Patera in [6] for coupling spectral element method and finite element methods. The main characteristic of such techniques is that the meshes on adjacent subdomains do not match across subdomain interfaces, allowing for the mesh on each subdomain to be generated independently of the rest of the domain. The coupling between adjacent subdomain meshes is done by requiring the jump in the finite element function across the subdomain interfaces to be orthogonal to some suitably chosen test space.

Since the introduction of the mortar concept, the techniques have been extensively studied by many authors. A saddle point formulation for the mortar technique was studied in [4]. Later, an extension to three dimensions was introduced in [5]. Further analysis and extensions of the mortar technique have been considered in [12,13,29,32,36,37]. Meanwhile, a number of efficient methods have been developed in order to solve the algebraic system resulting from the mortar discretization, including, e.g., substructuring methods [1,22], multigrid methods [14,26], additive Schwarz methods [9,21], hierarchical methods [16], but only a few of them have actually considered the case of jumping coefficients.

The purpose of this paper is to consider the nonconforming P1 element, also known as the lowest order Crouzeix-Raviart element, on nonmatching grids and develop an efficient additive Schwarz method for the corresponding algebraic system. The mortar technique for the nonconforming P1 element was analyzed by Marcinkowski in [29]. Even though, there exists a lot of work concerning the nonconforming P1 element on standard grids, cf., e.g., [15,19,20,27,28,30,31,38], the work on nonmatching grids is very limited, cf., e.g., [29,34,40].

The variants of the additive Schwarz method, which we introduce in this paper, follow the same idea as the one used for the conforming P1 finite element in [9]. The motivations for considering the nonconforming P1 finite element are several. First of all, there is a close relationship between mixed methods and nonconforming finite element methods for second order elliptic problems, cf., e.g., [2,3]. This relationship was further exploited for deriving efficient solvers for the mixed formulation [17]. The other known fact is the regular sparsity structure of the resulting stiffness matrices, which makes it easy for storage and writing efficient codes. The

final and the foremost motivation is the fact that there are no degrees of freedom associated with the nodes on the interface boundaries, which is a clear advantage over [9] with respect to analysis and implementation.

2 The discrete problem

Let $\Omega \subset \mathbb{R}^2$ be a bounded, simply connected polygonal domain, and let $\overline{\Omega} = \cup_{i=1}^N \overline{\Omega}_i$ be a partition into nonoverlapping polygonal subdomains Ω_i . We consider the following problem: Find $u^* \in H_0^1(\Omega)$ such that

$$a(u^*, v) = f(v), \quad v \in H_0^1(\Omega), \tag{1}$$

where

$$a(u, v) = \sum_{i=1}^N \rho_i (\nabla u, \nabla v)_{L^2(\Omega_i)} \quad \text{and} \quad f(v) = \sum_{i=1}^N \int_{\Omega_i} f v \, dx.$$

The coefficients $\rho_i, 1 \leq i \leq N$, are positive constants with large jumps across subdomain interfaces. We remark that the proposed method can also be used for problems where the coefficients ρ_i depend on x and are discontinuous only across subdomain interfaces. In this case the constant ρ_i can be taken as an average of $\rho_i(x)$ over the subdomain Ω_i .

We only consider the geometrically conforming case, i.e., the intersection between the closure of two different subdomains is either empty, a vertex, or an edge. The subdomains together form a coarse triangulation of the whole domain Ω with mesh size of order H_i , where H_i is the diameter of Ω_i . With each subdomain Ω_i , we associate a quasi-uniform triangulation $\mathcal{T}_h(\Omega_i)$ with mesh size of order h_i . The resulting triangulation can be nonmatching across subdomain interfaces. We use $\mathcal{T}_h(\partial\Omega_i)$ to denote the set of all triangles $\tau \in \mathcal{T}_h(\Omega_i)$ along $\partial\Omega_i$, such that $\partial\tau \cap \partial\Omega_i \neq \emptyset$. In the same way, $\mathcal{T}_h(\gamma_{m(i)})$ denotes the set of triangles along the mortar side $\gamma_{m(i)}$. We assume that the coarse triangulation and the triangulation of each subdomain are shape regular in the sense of [18].

For $D_i \subseteq \overline{\Omega}_i$, we refer to $\mathcal{N}_h(D_i)$ as the set of vertices and to $\mathcal{E}_h(D_i)$ as the set of edges of the triangulation $\mathcal{T}_h(\Omega_i)$ in D_i . For $E \in \mathcal{E}_h(D_i)$, we refer to $\text{mid}(E)$ as the midpoint of E . Further, $P_k(D_i), k \in \mathbb{N}_0$, stands for the set of polynomials of degree less than or equal to k on D_i . We denote by

$$\begin{aligned} X_h(\Omega_i) &:= \{v \in L^2(\Omega_i) \mid v|_\tau \in P_1(\tau), \tau \in \mathcal{T}_h(\Omega_i), \\ &\quad v \text{ is continuous in } \text{mid}(E), E \in \mathcal{E}_h(\Omega_i), \\ &\quad v(\text{mid}(E)) = 0, E \in \mathcal{E}_h(\partial\Omega_i \cap \partial\Omega)\} \end{aligned}$$

the nonconforming P1 (Crouzeix-Raviart) finite element space defined on the triangulation $\mathcal{T}_h(\Omega_i)$ of Ω_i . For notational convenience, in the sequel we will refer to $\Omega_{ih} := \mathcal{N}_h(\Omega_i)$ and $\partial\Omega_{ih} := \mathcal{N}_h(\partial\Omega_i)$ as the sets of vertices, i.e., conforming P1 nodal points, in Ω_i and $\partial\Omega_i$. Likewise, the sets $\Omega_{ih}^{CR} := \{\text{mid}(E) \mid E \in \mathcal{E}_h(\Omega_i)\}$ and $\partial\Omega_{ih}^{CR} := \{\text{mid}(E) \mid E \in \mathcal{E}_h(\partial\Omega_i)\}$ stand for the sets of midpoints of edges, i.e., the

nonconforming P1 (Crouzeix-Raviart) nodal points, in Ω_i and $\partial\Omega_i$, respectively. Using $X_h(\Omega_i)$, we define the product space X_h on the whole domain as

$$X_h(\Omega) = X_h(\Omega_1) \times X_h(\Omega_2) \cdots \times X_h(\Omega_N).$$

Let Γ_{ij} be an open edge common to Ω_i and Ω_j , i.e., $\bar{\Gamma}_{ij} = \bar{\Omega}_i \cap \bar{\Omega}_j$. Note that each interface Γ_{ij} inherits two different discretizations from its two sides. We select one side of Γ_{ij} as the master side, called the mortar, and the other side as the slave side, called the nonmortar. We define the skeleton $\mathcal{S} = (\bigcup_{i=1}^N \partial\Omega_i) \setminus \partial\Omega$ of the decomposition as follows:

$$\bar{\mathcal{S}} = \bigcup_m \bar{\gamma}_m, \quad \text{with } \gamma_m \cap \gamma_n = \emptyset \text{ if } m \neq n,$$

where each γ_m denotes an open mortar edge. We write γ_m as $\gamma_{m(i)}$, if it is an edge of Ω_i , i.e., $\gamma_{m(i)} \subset \partial\Omega_i$. Let $\delta_m = \delta_{m(j)} \subset \partial\Omega_j$ be the corresponding open nonmortar edge of Ω_j that occupies the same geometrical space as $\gamma_{m(i)}$, i.e., $\gamma_{m(i)} = \Gamma_{ij} = \delta_{m(j)}$ (See Figure 1 for an illustration).

Since the triangulations on Ω_i and Ω_j do not match on their common interface Γ_{ij} , the functions of $X_h(\Omega)$ are discontinuous at the set of edge midpoints $\gamma_{m(i)h}^{CR} := \{\text{mid}(E) \mid E \in \mathcal{E}_h(\gamma_{m(i)})\}$ on the mortar side $\gamma_{m(i)}$, or $\delta_{m(j)h}^{CR} := \{\text{mid}(E) \mid E \in \mathcal{E}_h(\delta_{m(j)})\}$ on the nonmortar side $\delta_{m(j)}$. A weak continuity condition, called the mortar condition, is therefore imposed (cf. [29]). Let $u_h \in X_h$, where $u_h = \{u_i\}_{i=1}^N$. A function $u_h \in X_h$ satisfies the mortar condition on $\delta_{m(j)} = \Gamma_{ij} = \gamma_{m(i)}$, if

$$Q_m u_i = Q_m u_j, \tag{2}$$

where $Q_m : L^2(\Gamma_{ij}) \rightarrow M^{hj}(\delta_{m(j)})$ is the L^2 -projection operator defined as:

$$(Q_m u, \psi)_{L^2(\delta_{m(j)})} = (u, \psi)_{L^2(\delta_{m(j)})}, \quad \forall \psi \in M^{hj}(\delta_{m(j)}), \tag{3}$$

where $M^{hj}(\delta_{m(j)}) \subset L^2(\Gamma_{ij})$ is the test space of functions which are piecewise constant on the triangulation of $\delta_{m(j)}$, and $(\cdot, \cdot)_{L^2(\delta_{m(j)})}$ denotes the L^2 inner product on $L^2(\delta_{m(j)})$.

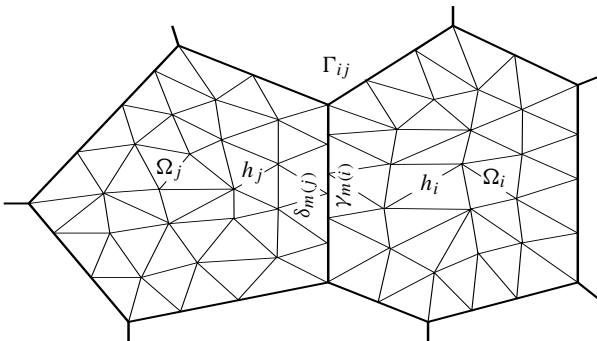


Fig. 1 A mortar- ($\gamma_{m(i)}$) and a nonmortar- ($\delta_{m(j)}$) side of a subdomain interface (Γ_{ij}) with non-matching meshes on both sides

The finite element space $V_h \subset X_h$ is the subspace of functions which satisfy the mortar condition for all $\delta_m \subset \mathcal{S}$. We denote by ψ_x the basis function of V_h with supporting edge midpoint $x \in \left(\bigcup_{\gamma_{m(i)} \subset \partial\Omega_i} \gamma_{m(i)h}^{CR} \right) \cup \Omega_{ih}^{CR}$, $i = 1, \dots, N$, cf. [29]. The values at the edge midpoints of $\delta_{m(j)h}^{CR}$ are determined by using the mortar condition. We note that, for a mortar side $\gamma_{m(i)}$, the basis functions associated with some of the edge midpoints of Ω_{ih}^{CR} may have support on the corresponding nonmortar side $\delta_{m(j)}$. These edge midpoints in Ω_{ih}^{CR} are exactly the edge midpoints that belong to the same triangles as those of $\gamma_{m(i)h}^{CR}$. We denote the set of these edge midpoints, corresponding to the mortar side $\gamma_{m(i)}$, by $v_{m(i)h}^{CR}$, i.e., $v_{m(i)h}^{CR} := \{x \in \Omega_{ih}^{CR} \mid \text{supp } \psi_x \cap \delta_{m(j)} \neq \emptyset\}$, where $\gamma_{m(i)} = \delta_{m(j)}$. Note that $v_{m(i)h}^{CR}$ and $\gamma_{m(i)h}^{CR}$ are two disjoint sets. The union of the sets $v_{m(i)h}^{CR}$, for all mortar sides $\gamma_{m(i)} \subset \partial\Omega_i$, is denoted by v_{ih}^{CR} , i.e., $v_{ih}^{CR} := \bigcup_{\gamma_{m(i)} \subset \partial\Omega_i} v_{m(i)h}^{CR}$. We note that the situation in the conforming P1 case is different from the one described here. In the conforming P1 case, the basis functions associated with interior nodal points, do not have supports on the nonmortar side, and so we have to take into consideration this difference when extending a method from the conforming P1 case to the nonconforming P1 case.

From the definition of the finite element space V_h , the value of its any function u on the nonmortar side is determined from values on the mortar side. Accordingly, if we let a cross point x_c , cf. Figure 2 (left), be a vertex of only one triangle inside each of the subdomains sharing the cross point, and choose the mortar and nonmortar sides such that $h_\delta^c < h_\gamma^c$ for all mortar and nonmortar sides meeting at the cross point, where h_γ^c and h_δ^c denote the lengths of the triangle edges touching the cross point from the mortar and the nonmortar sides, respectively, then it is not difficult to see, using the mortar condition, that the value on a nonmortar side will have to depend on the value itself. This creates a deadlock situation which is unsolvable, and hence this particular combination of h_γ^c, h_δ^c and the mortar sides cannot form a valid choice. However, if the cross point is a vertex of at least two triangles in any one of those sharing subdomains, this deadlock breaks (anti-deadlock), and any combination of mortar sides will give a valid choice. A common practice for triangulation, however, is to have always two triangles sharing a corner point, cf. Figure 2 (right).

Since functions of V_h are not continuous, we use the broken bilinear form $a_h(\cdot, \cdot)$ defined according to

$$a_h(u, v) = \sum_{i=1}^N a_i(u, v) = \sum_{i=1}^N \rho_i \sum_{\tau \in \mathcal{T}_h(\Omega_i)} (\nabla u, \nabla v)_{L^2(\tau)}.$$

The discrete problem takes the following form: Find $u_h^* = \{u_i\}_{i=1}^N \in V_h$ such that

$$a_h(u_h^*, v_h) = f(v_h), \quad \forall v_h \in V_h. \tag{4}$$

V_h is a Hilbert space with an inner product defined by $a_h(u_h, v_h)$. The problem has a unique solution and a priori error estimates have been provided in [29].

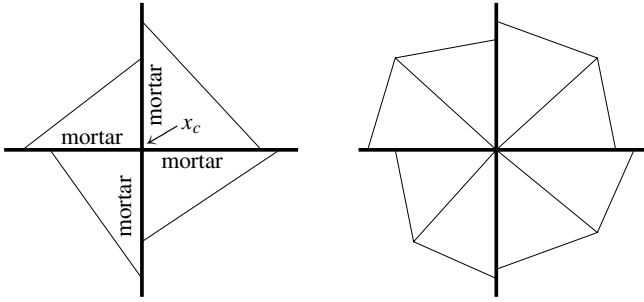


Fig. 2 Triangles around the cross point x_c illustrating a deadlock situation, for the choice of mortar and nonmortar sides, on the left, and an anti-deadlock situation on the right

3 The additive Schwarz method

In this section, we design an additive Schwarz method for the problem (4), the basic idea of which is similar to the ones in [11] for the conforming P1 element, and in [9] for the conforming P1 mortar element. For simplicity, we assume that each cross point is a vertex of at least two triangles inside each of its subdomains sharing it, cf. Figure 2 (right). The algorithm is easily extendable to the single triangle case. The method is defined using the general framework for additive Schwarz methods [33], i.e., in terms of a decomposition of the global space V_h into subspaces and the bilinear forms defined on these subspaces. We decompose V_h into smaller subspaces by means of

$$V_h = V^S + V^0 + \sum_{i=1}^N V^i. \tag{5}$$

We note that V^i , $1 \leq i \leq N$, is the restriction of V_h to Ω_i with functions vanishing at $\partial\Omega_{ih}^{CR}$, and v_{ih}^{CR} , as well as on the remaining subdomains. V^S is a space of functions given by their values on $S_h^{CR} = \bigcup_{\gamma_m \subset S} \{\gamma_{mh}^{CR} \cup v_{mh}^{CR}\}$, and V^0 is a coarse space having a dimension equal to the number of subdomains. The space V^S is defined as follows:

$$V^S = \left\{ v \in V_h : v(x) = 0, x \in \bigcup_{i=1}^N \{\Omega_{ih}^{CR} \setminus v_{ih}^{CR}\} \right\}. \tag{6}$$

For the specification of the coarse space V^0 , we provide the notion of connectedness of CR nodal points.

Definition 1 We say that a CR nodal point x is connected to the subdomain Ω_i if $x \in \overline{\Omega_{ih}^{CR}}$. If the CR nodal point $x \in \gamma_{m(i)h}^{CR} \cup v_{m(i)h}^{CR}$ then x is said to be connected to both Ω_i and Ω_j where $\gamma_{m(i)} = \delta_{m(j)}$. In other words, the CR nodal point x is connected to Ω_i if and only if the basis function of V_h , associated with the nodal point x , has a nonzero support in Ω_i .

By making each cross point to be shared by at least two triangles within each subdomain, the maximum number of subdomains a CR nodal point can be connected to, in the two dimensional case, is three. Let χ_i , associated with the subdomain Ω_i , be the function belonging to the space $X_h(\Omega_i)$, defined by its nodal values at $x \in \overline{\Omega}_{ih}^{CR}$. For each such nodal point x

$$\chi_i(x) = \frac{1}{\sum_j \rho_j(x)},$$

where the sum is taken over the subdomains that x is connected to (in the sense of Definition 1). Note that for $\rho_i = \rho_j = 1$, χ_i is 1 at $x \in \Omega_{ih}^{CR} \setminus v_{ih}^{CR}$, 1 at $x \in \delta_{m(i)h}^{CR}$, and $\frac{1}{2}$ at $x \in \gamma_{m(i)h}^{CR}$. χ_i is $\frac{1}{2}$ at $x \in v_{m(i)h}^{CR} \cup v_{n(i)h}^{CR}$ except those which belong to both sets $v_{m(i)h}^{CR}$ and $v_{n(i)h}^{CR}$, in which case χ_i is $\frac{1}{3}$.

We partition the set of subdomains Ω_i , $1 \leq i \leq N$, into two subsets, the set of interior subdomains N_I and the set of boundary subdomains N_B . Subdomains belonging to N_B contain at least an edge lying on $\partial\Omega$ while those of the interior set N_I do not.

We associate with each subdomain Ω_i the sets G_i containing the indices of its neighboring subdomains defined as follows: G_i contains the index j of a neighbor Ω_j if it shares an edge Γ_{ij} ($\Gamma_{ij} = \overline{\Omega}_i \cap \overline{\Omega}_j$) with Ω_i .

We are now ready to define the coarse space V^0 which is given as the span of its basis functions, Φ_i , $1 \leq i \leq N$, i.e.,

$$V^0 = span \{ \Phi_i : i = 1, \dots, N \}. \tag{7}$$

Each function Φ_i , associated with the subdomain Ω_i , is a function in the finite element space V_h .

For an interior subdomain Ω_i ($\Omega_i \in N_I$) (cf. Figure 3), the function Φ_i is constructed in two steps. We first define Φ_i on $\overline{\Omega}_i$ and then on $\overline{\Omega}_j$ where $i \in G_j$.

(i) Φ_i on $\overline{\Omega}_i$ (cf. Figure 3) is given as

$$\Phi_i(x) = \begin{cases} 1, & x \in \Omega_{ih}^{CR} \setminus v_{ih}^{CR}, \\ \rho_i \chi_i(x), & x \in \gamma_{m(i)h}^{CR} \cup v_{m(i)h}^{CR}, \\ \rho_i Q_m(\chi_j)(x), & x \in \delta_{m(i)h}^{CR}, \delta_{m(i)} = \gamma_{m(j)}. \end{cases} \tag{8}$$

(ii) Φ_i on $\overline{\Omega}_j$ (cf. Figure 3), where $i \in G_j$, is given as

$$\Phi_i(x) = \begin{cases} \rho_i Q_m(\chi_i)(x), & x \in \delta_{m(j)h}^{CR}, \delta_{m(j)} = \gamma_{m(i)}, \\ \rho_i \chi_j(x), & x \in \gamma_{m(j)h}^{CR} \cup v_{m(j)h}^{CR}, \gamma_{m(j)} = \delta_{m(i)}, \\ 0, & \text{at all other } x \text{ in } \overline{\Omega}_{jh}^{CR}. \end{cases} \tag{9}$$

On the remaining subdomains, at all edge midpoints, $\Phi_i = 0$. This completes the definition of Φ_i for Ω_i .

If Ω_i is a boundary subdomain ($\Omega_i \in N_B$) then the function Φ_i is defined as above with the following additional condition.

$$\Phi_i(x) = 0, \quad x \in \partial\Omega_{ih}^{CR} \cap \partial\Omega. \tag{10}$$

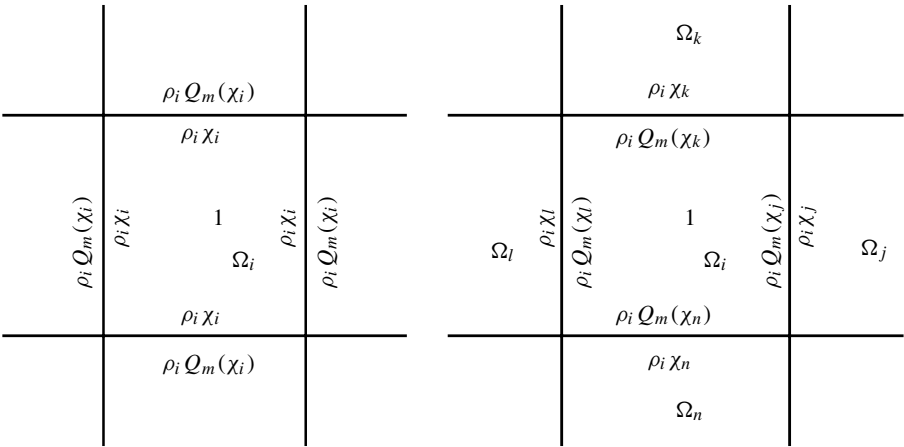


Fig. 3 Illustrations of the basis function Φ_i associated with an interior subdomain Ω_i , indicating the subdomain interior, the mortar sides, and the nonmortar sides where the function takes nonzero values. On the left, Ω_i only has mortar sides, and on the right, Ω_i only has nonmortar sides

Remark 1 The functions Φ_i have the property that $\Phi_i(x) + \sum_{j \neq i} \Phi_j(x) = 1$ at all $x \in \bar{\Omega}_i$, where $\Omega_i \in N_I$. For $\Omega_i \in N_B$, this equality is true everywhere in $\bar{\Omega}_i$ except for the triangles having at least an edge lying on the boundary $\partial\Omega$.

Remark 2 Following the definition of $\chi_i \in X_h(\Omega_i)$, it is easy to see that $\rho_i \chi_i(x) = 1$ at $x \in \Omega_{ih}^{CR} \setminus v_{ih}^{CR}$, and $\rho_i \chi_i(x) < 1$ and $\rho_j \chi_j(x) < 1$ at $x \in \gamma_{m(i)h}^{CR} \cup v_{m(i)h}^{CR}$. Consequently $\rho_i \rho_j \chi_i^2(x) < 1$ at $x \in \gamma_{m(i)h}^{CR} \cup v_{m(i)h}^{CR}$.

We use exact bilinear forms for all our subproblems, i.e., we define $b^i(\cdot, \cdot) : V^i \times V^i \rightarrow \Re$ for $i \in \{S, 0, \dots, N\}$ as

$$b^i(u, v) = a_h(u, v), \quad u, v \in V^i. \tag{11}$$

For $1 \leq i \leq N$, any function $u \in V^i$ is of the form $u = \{u_j\}_{j=1}^N$ where $u_j = 0$ for $j \neq i$. Hence, for $1 \leq i \leq N$, we have

$$a_h(u, v) = a_i(u_i, v_i), \quad u, v \in V^i. \tag{12}$$

The projection like operators $T^i : V_h \rightarrow V^i$ are defined in the standard way, i.e., for $i \in \{S, 0, \dots, N\}$ and $u \in V_h$, $T^i u \in V^i$ is the solution of

$$b^i(T^i u, v) = a_h(u, v), \quad v \in V^i. \tag{13}$$

Note that, for $1 \leq i \leq N$, problem (13) reduces to a Dirichlet problem on Ω_i with homogeneous boundary condition. To compute the corresponding stiffness matrices, we need the standard nodal basis functions $\varphi_i^{(k)}$ associated with $x_k \in \Omega_{ih}^{CR} \setminus v_{ih}^{CR}$ only. For $i \in \{S, 0\}$, problem (13) is a coarse space problem.

Let

$$T = T^S + T^0 + T^1 + \dots + T^N.$$

Problem (4) is now replaced by the following preconditioned system,

$$Tu^* = g, \tag{14}$$

where $g = T^S u^* + \sum_{i=0}^N T^i u^*$. Note that $T^i u^*$ can be calculated without knowing u^* , the solution of (4) (cf., e.g., [33]).

3.1 Analysis

Let $\mathcal{T}_{\frac{h}{2}}(\Omega_i)$ be another triangulation associated with the subdomain Ω_i which is obtained as a result of joining the midpoints of the edges of the elements of $\mathcal{T}_h(\Omega_i)$. Let $W_{\frac{h}{2}}(\Omega_i)$ be the conforming space of piecewise linear continuous functions on the triangulation $\mathcal{T}_{\frac{h}{2}}(\Omega_i)$. The functions of this space are defined by their values at the set $\overline{\Omega}_{i, \frac{h}{2}}$ of all triangle vertices of $\mathcal{T}_{\frac{h}{2}}(\Omega_i)$. It is easy to see that $\overline{\Omega}_{i, \frac{h}{2}} = \overline{\Omega}_{ih}^{CR} \cup \overline{\Omega}_{ih}$. We introduce the local equivalence mapping $\mathcal{M}_i : X_h(\Omega_i) \rightarrow W_{\frac{h}{2}}(\Omega_i)$ as defined in [31].

Definition 2 For $u \in X_h(\Omega_i)$,

$$\mathcal{M}_i u(x) = \begin{cases} u(x), & x \in \overline{\Omega}_{ih}^{CR}, \\ \frac{1}{n_x} \sum_{\tau \in \mathcal{T}_x} u|_{\tau}(x), & x \in \Omega_{ih}, \\ \frac{|x_l x|}{|x_l x_r|} u(x_l) + \frac{|x x_r|}{|x_l x_r|} u(x_r), & x \in \partial\Omega_{ih}. \end{cases} \tag{15}$$

Here, \mathcal{T}_x is the set of elements sharing the common vertex x . n_x denotes the number of such elements. x_l and x_r are the left- and the right neighboring edge midpoints of x , respectively.

The properties of such equivalence mapping are given in the following lemma. For a proof we refer to [29, 31].

Lemma 1 Let $\mathcal{M}_i : X_h(\Omega_i) \rightarrow W_{\frac{h}{2}}(\Omega_i)$ be the local equivalence mapping as defined above. Then, for all $u \in X_h(\Omega_i)$ there holds

$$|\mathcal{M}_i u|_{H^1(\Omega_i)} \leq c |u|_{h,1(\Omega_i)}, \tag{16}$$

$$\|u - \mathcal{M}_i u\|_{L^2(\Omega_i)} \leq c h_i |u|_{h,1(\Omega_i)}, \tag{17}$$

$$\|u - \mathcal{M}_i u\|_{L^2(\Gamma)} \leq c h_i^{1/2} |u|_{h,1(\Omega_i)}, \tag{18}$$

where $|u|_{h,1(\Omega_i)}^2 = \sum_{\tau \in \mathcal{T}_h(\Omega_i)} |u|_{H^1(\tau)}^2$, and Γ is an edge of Ω_i .

Lemma 2 For $u = \{u_i\}_{i=1}^N \in V_h$, let $u^0 = \sum_{i=1, \dots, N} \alpha_i \Phi_i$, where α_i is the average of $\mathcal{M}_i u_i$ over $\partial\Omega_i$, i.e., $\alpha_i = \frac{1}{|\partial\Omega_i|} \int_{\partial\Omega_i} \mathcal{M}_i u_i ds$. We have

$$a_h(u^0, u^0) \leq c \frac{H}{h} a_h(u, u) \tag{19}$$

and

$$\sum_{i=1}^N \rho_i h_i^{-1} \|u^0 - \alpha_i\|_{L^2(\Omega_i)}^2 \leq c H a_h(u, u), \tag{20}$$

where c is a positive constant independent of the mesh sizes $h = \inf_i h_i$ and $H = \max_i H_i$, and of the jumps of the coefficients ρ_i .

Proof The outline of the proof is as follows: We first prove (19) and then show how (20) can be derived from (19). For the proof, we look at each subdomain at a time. Moreover, we treat the interior and the boundary subdomains separately.

(i) Interior subdomain

Let $\Omega_i \in N_I$ be an interior subdomain. u^0 on $\bar{\Omega}_i$ can be written as

$$u^0 = \alpha_i \Phi_i + \sum_{j \in G_i} \alpha_j \Phi_j.$$

It follows from the definition of u^0 and Remark 1 that

$$u^0 - \alpha_i = \sum_{j \in G_i} (\alpha_j - \alpha_i) \Phi_j \quad \text{on } \bar{\Omega}_i,$$

whence

$$\begin{aligned} a_i(u^0, u^0) &= a_i(u^0 - \alpha_i, u^0 - \alpha_i) \\ &\leq c \sum_{j \in G_i} \rho_i (\alpha_j - \alpha_i)^2 \sum_{\tau \in \mathcal{T}_h(\Omega_i)} |\Phi_j|_{H^1(\tau)}^2. \end{aligned} \tag{21}$$

In order to find an estimate for the right hand side above, we try to estimate the term $(\alpha_j - \alpha_i)^2$ first. We refer to \bar{u}_Γ as the average of $u \in L^2(\Gamma)$ over the edge Γ , i.e. $\bar{u}_\Gamma = \frac{1}{|\Gamma|} \int_\Gamma u \, ds$. We note that, for any function $u = \{u_i\}_{i=1}^N \in V_h$, $\overline{(u_i)}_{\gamma_{m(i)}} = \overline{(u_j)}_{\delta_{m(j)}}$ where $\gamma_{m(i)} = \delta_{m(j)}$. Hence,

$$\begin{aligned} (\alpha_j - \alpha_i)^2 &\leq c \left\{ \left(\alpha_j - \overline{(\mathcal{M}_j u_j)}_{\delta_{m(j)}} \right)^2 + \left(\overline{(\mathcal{M}_j u_j)}_{\delta_{m(j)}} - \overline{(u_j)}_{\delta_{m(j)}} \right)^2 \right. \\ &\quad \left. + \left(\overline{(u_i)}_{\gamma_{m(i)}} - \overline{(\mathcal{M}_i u_i)}_{\gamma_{m(i)}} \right)^2 + \left(\alpha_i - \overline{(\mathcal{M}_i u_i)}_{\gamma_{m(i)}} \right)^2 \right\} \end{aligned}$$

Following the lines of the proof of the first lemma in [9], and using (16), we can bound the first and the last terms inside the curly brackets above, by $c|u_j|_{h,1(\Omega_j)}^2$ and $c|u_i|_{h,1(\Omega_i)}^2$, respectively. The second and the fourth terms can be estimated

using the Cauchy-Schwarz inequality and (18). Below, we derive explicitly the estimate for the second term only, as for the fourth term it is then straightforward.

$$\begin{aligned} \left(\overline{(u_i)}_{\gamma_{m(i)}} - \overline{(\mathcal{M}_i u_i)}_{\gamma_{m(i)}} \right)^2 &= \left(\overline{(u_i - \mathcal{M}_i u_i)}_{\gamma_{m(i)}} \right)^2 \\ &\leq c \frac{1}{H_i} \| u_i - \mathcal{M}_i u_i \|_{L^2(\gamma_{m(i)})}^2 \\ &\leq c |u_i|_{h,1(\Omega_i)}^2. \end{aligned}$$

Similarly, for the fourth term, we have $\left(\overline{(u_j)}_{\delta_{m(j)}} - \overline{(\mathcal{M}_j u_j)}_{\delta_{m(j)}} \right)^2 \leq c |u_j|_{h,1(\Omega_j)}^2$. Hence,

$$(\alpha_j - \alpha_i)^2 \leq c \left\{ |u_i|_{h,1(\Omega_i)}^2 + |u_j|_{h,1(\Omega_j)}^2 \right\}. \tag{22}$$

The inverse inequality yields

$$\rho_i \sum_{\tau \in \mathcal{T}_h(\Omega_i)} |\Phi_j|_{H^1(\tau)}^2 \leq c \rho_i \sum_{\tau \in \mathcal{T}_h(\Gamma_{ij})} h_\tau^{-2} \| \Phi_j \|_{L^2(\tau)}^2 \tag{23}$$

since Φ_j is zero at all triangles $\tau \in \mathcal{T}_h(\Omega_i)$ except those in $\mathcal{T}_h(\Gamma_{ij})$, where $\Gamma_{ij} \subset \partial\Omega_i$ is either a mortar or a nonmortar.

If $\Gamma_{ij} = \overline{\Omega}_i \cup \overline{\Omega}_j$ is a mortar $\gamma_{m(i)}$ in Ω_i , by definition of the basis functions (cf. (9)) we have

$$\Phi_j(x) = \rho_j \chi_i(x) \quad \text{at } x \in \gamma_{m(i)h}^{CR} \cup \nu_{m(i)h}^{CR}. \tag{24}$$

Using (24) and the fact that $\rho_j \chi_i(x) < 1$ and $\rho_i \rho_j \chi_i^2(x) < 1$, for all $x \in \gamma_{m(i)h}^{CR} \cup \nu_{m(i)h}^{CR}$, cf. Remark 2, we obtain

$$\begin{aligned} \rho_i \sum_{\tau \in \mathcal{T}_h(\gamma_{m(i)})} h_\tau^{-2} \| \Phi_j \|_{L^2(\tau)}^2 &\leq c \rho_i \sum_{x \in \gamma_{m(i)h}^{CR} \cup \nu_{m(i)h}^{CR}} \rho_j^2 \chi_i^2(x) \\ &\leq c \min(\rho_i, \rho_j) \frac{H_i}{h_i}. \end{aligned} \tag{25}$$

On the other hand, if Γ_{ij} is a nonmortar $\delta_{m(i)}$ in Ω_i , we get (cf. (9)),

$$\Phi_j(x) = \rho_j Q_m(\chi_j)(x) \quad \text{at } x \in \delta_{m(i)h}^{CR}. \tag{26}$$

We observe that Φ_j is piecewise constant on $\delta_{m(i)}$. In view of (26), the L^2 -stability of the projection operator Q_m (cf. [29]), i.e.,

$$\| Q_m(\chi_j) \|_{L^2(\delta_{m(i)})} \leq c \| \chi_j \|_{L^2(\gamma_{m(j)})},$$

and the fact that $\rho_j \chi_j(x) < 1$ and $\rho_i \rho_j \chi_j^2(x) < 1$, for $x \in \gamma_{m(j)h}^{CR} \cup \nu_{m(j)h}^{CR}$, cf. Remark 2, we arrive at

$$\begin{aligned}
 \rho_i \sum_{\tau \in \mathcal{T}_h(\delta_{m(i)})} h_\tau^{-2} \|\Phi_j\|_{L^2(\tau)}^2 &\leq c \rho_i \sum_{x \in \delta_{m(i)h}^{CR}} \Phi_j^2(x) \\
 &\leq c \rho_i h_i^{-1} \|\rho_j \mathcal{Q}_m(\chi_j)\|_{L^2(\delta_{m(i)})}^2 \\
 &\leq c \rho_i h_i^{-1} \|\rho_j \chi_j\|_{L^2(\gamma_{m(j)})}^2 \\
 &\leq c \rho_i h_i^{-1} h_j \sum_{x \in \gamma_{m(j)h}^{CR} \cup \nu_{m(j)h}^{CR}} \rho_j^2 \chi_j^2(x) \\
 &\leq c \min(\rho_i, \rho_j) \frac{H_j}{h_i}. \tag{27}
 \end{aligned}$$

Hence, combining (21)–(27), for $\Omega_i \in N_I$, we have

$$a_i(u^0, u^0) \leq c \frac{H}{h} \left\{ a_i(u_i, u_i) + \sum_{j \in G_i} a_j(u_j, u_j) \right\}. \tag{28}$$

(ii) *Boundary subdomain*

In case when $\Omega_i \in N_B$ is a boundary subdomain ($\Omega_i \in N_B$), we introduce an auxiliary function \hat{u}^0 by means of

$$\hat{u}^0 = \sum_{\Omega_i \in N_I} \alpha_i \hat{\Phi}_i + \sum_{\Omega_i \in N_B} \alpha_i \hat{\Phi}_i,$$

where the function $\hat{\Phi}_i$, $\Omega_i \in N_B$, is defined as follows: Let $\{\hat{\Phi}_i\}_{\Omega_i \in N_B}$ be the set of functions constructed in exactly the same way as the functions Φ_i associated with the interior subdomains, are constructed assuming that any edge of $\Omega_i \in N_B$ which lies on the boundary $\partial\Omega$ is a mortar in Ω_i . Accordingly, $\hat{\Phi}_i(x) = 1$ at $x \in \partial\Omega_{ih}^{CR} \cap \partial\Omega$.

On $\bar{\Omega}_i$, the function \hat{u}^0 takes the form

$$\hat{u}^0 = \alpha_i \hat{\Phi}_i + \sum_{j \in G_i, \Omega_j \in N_I} \alpha_j \Phi_j + \sum_{j \in G_i, \Omega_j \in N_B} \alpha_j \hat{\Phi}_j.$$

Obviously,

$$a_i(u^0, u^0) \leq 2 \{a_i(u^0 - \hat{u}^0, u^0 - \hat{u}^0) + a_i(\hat{u}^0, \hat{u}^0)\}. \tag{29}$$

On $\bar{\Omega}_i$, the function \hat{u}^0 has the same form as u^0 on an interior subdomain. Therefore, the second term can be estimated as in (28). For the first term, we note that $\hat{\Phi}_j = \Phi_j$ on $\bar{\Omega}_i$. Hence, we get

$$(u^0 - \hat{u}^0) = \alpha_i (\Phi_i - \hat{\Phi}_i) \quad \text{on } \bar{\Omega}_i.$$

Consequently,

$$\begin{aligned}
 a_i(u^0 - \hat{u}^0, u^0 - \hat{u}^0) &= \rho_i \sum_{\tau \in \mathcal{T}_h(\Omega_i)} |u^0 - \hat{u}^0|_{H^1(\tau)}^2 \\
 &\leq c\rho_i \alpha_i^2 \sum_{\tau \in \mathcal{T}_h(\Omega_i)} |\Phi_i - \hat{\Phi}_i|_{H^1(\tau)}^2.
 \end{aligned} \tag{30}$$

Observing that $\mathcal{M}_i u_i$ is zero on a boundary edge of Ω_i , a simple trace inequality and Friedrichs' inequality yield

$$\begin{aligned}
 \alpha_i^2 &= \left\{ \frac{1}{|\partial\Omega_i|} \int_{\partial\Omega_i} \mathcal{M}_i u_i \, ds \right\}^2 \leq cH_i^{-1} \| \mathcal{M}_i u_i \|_{L^2(\partial\Omega_i)}^2 \\
 &\leq c|\mathcal{M}_i u_i|_{H^1(\Omega_i)}^2 \\
 &\leq c|u_i|_{h,1(\Omega_i)}^2.
 \end{aligned} \tag{31}$$

Using the inverse inequality, we get

$$\begin{aligned}
 \rho_i \sum_{\tau \in \mathcal{T}_h(\Omega_i)} |\Phi_i - \hat{\Phi}_i|_{H^1(\tau)}^2 &\leq c\rho_i \sum_{\tau \in \mathcal{T}_h(\partial\Omega_i)} h_\tau^{-2} \| \Phi_i - \hat{\Phi}_i \|_{L^2(\tau)}^2 \\
 &\leq c\rho_i \sum_{x \in \partial\Omega_{ih}^{CR}} (\Phi_i(x) - \hat{\Phi}_i(x))^2 \\
 &= c\rho_i \sum_{x \in \partial\Omega_{ih}^{CR} \cap \partial\Omega} \hat{\Phi}_i^2(x) \\
 &\leq c\rho_i \frac{H_i}{h_i},
 \end{aligned} \tag{32}$$

where we have used the fact that $\Phi_i(x) = \hat{\Phi}_i(x)$ at all $x \in \overline{\Omega_{ih}^{CR}} \setminus \partial\Omega$, and that $\hat{\Phi}_i(x) = 1$ at all $x \in \partial\Omega_{ih}^{CR} \cap \partial\Omega$.

Now, combining the inequalities (30)–(32) and replacing the resulting estimate together with the estimate (the same as in (28)) for $a_i(\hat{u}^0, \hat{u}^0)$ in (29), we obtain a similar bound as (28). Since the subdomains are shape regular, the maximal number of neighbors in G_i can be bounded independently of the total number N of subdomains. The proof of (19) thus follows by summing (28) over all subdomains.

(iii) Proof of (20)

For $\Omega_i \in N_I$, we have

$$\rho_i \| u^0 - \alpha_i \|_{L^2(\Omega_i)}^2 \leq c \sum_{j \in G_i} \rho_j (\alpha_j - \alpha_i)^2 \sum_{\tau \in \mathcal{T}_h(\Omega_i)} \| \Phi_j \|_{L^2(\tau)}^2,$$

where we have replaced the H^1 -seminorm with the L^2 -norm in (21). The estimate for $\| \Phi_j \|_{L^2(\Omega_i)}^2$ will gain a factor h_i^2 compared with $|\Phi_j|_{H^1(\Omega_i)}^2$ (cf. (25) and (27)).

This results in a factor $h_i H$ instead of $\frac{H}{h_i}$. If we now follow the same steps as in the proof of the first part of the lemma, we obtain

$$\rho_i \| u^0 - \alpha_i \|_{L^2(\Omega_i)}^2 \leq c h_i H \left\{ a_i(u_i, u_i) + \sum_{j \in G_i} a_j(u_j, u_j) \right\}. \tag{33}$$

For $\Omega_i \in N_B$, we use exactly the same arguments, which again leads to the factor $h_i H$ instead of $\frac{H}{h_i}$, and follow the same steps as in the proof of the first part of the lemma for $\Omega_i \in N_B$ to get the same estimate as (33). The proof of (20) thus follows by summing (33) over all subdomains. This concludes the proof of Lemma 2. \square

Theorem 1 *There exist positive constants c_0 and c_1 , independent of the mesh sizes $h = \inf_i h_i$ and $H = \max_i H_i$, and of the jumps of the coefficients ρ_i , such that for all $u \in V_h$*

$$c_0 \frac{h}{H} a_h(u, u) \leq a_h(Tu, u) \leq c_1 a_h(u, u). \tag{34}$$

Proof The proof relies on the general Schwarz framework (cf. [33]). According to the general Schwarz framework, the proof of the theorem follows as soon as the following three key assumptions are verified.

Assumption 1 *For all $u = \{u_i\}_{i=1}^N \in V_h$, there exists a splitting*

$$u = u^S + u^0 + \sum_{i=1}^N u^i,$$

and a constant c , independent of the mesh sizes h and H and of the jumps of the coefficients ρ_i , such that

$$b^S(u^S, u^S) + b^0(u^0, u^0) + \sum_{i=1}^N b^i(u^i, u^i) \leq c \frac{H}{h} a_h(u, u). \tag{35}$$

Proof of Assumption 1 For $u = \{u_i\}_{i=1}^N \in V_h$, we define $u^0 \in V^0$ as

$$u^0 = \sum_{i=1}^N \alpha_i \Phi_i,$$

where α_i and Φ_i , $1 \leq i \leq N$, are as defined before (cf. Lemma 2). Let $w = u - u^0 = \{w_i\}_{i=1}^N$ and let $u^S = \{u_i^S\}_{i=1}^N \in V^S$ be defined by the nodal values as follows

$$u_i^S(x) = \begin{cases} w_i(x), & x \in \partial\Omega_{ih}^{CR} \cup v_{ih}^{CR}, \\ 0, & x \in \Omega_{ih}^{CR} \setminus v_{ih}^{CR}. \end{cases}$$

Similarly, let $u^j = \{u_i^j\}_{i=1}^N \in V^j$, $1 \leq j \leq N$, be defined by the nodal values according to

$$u_j^j = \begin{cases} w_j(x), & x \in \Omega_{jh}^{CR} \setminus v_{jh}^{CR}, \\ 0, & x \in \partial\Omega_{jh}^{CR} \cup v_{jh}^{CR}, \end{cases}$$

with $u_i^j = 0$ for all $x \in \overline{\Omega}_{ih}^{CR}$ whenever $i \neq j$. Clearly, $u = u^S + \sum_{i=0}^N u^i$. We now use this splitting of u to prove Assumption 1.

For $u^S = \{u_i^S\}_{i=1}^N \in V^S$, we have

$$b^S(u^S, u^S) = \sum_{i=1}^N a_i(u_i^S, u_i^S). \tag{36}$$

In view of the inverse inequality we get

$$\begin{aligned} a_i(u_i^S, u_i^S) &= \rho_i \sum_{\tau \in \mathcal{T}_h(\Omega_i)} |u_i^S|_{H^1(\tau)}^2 \\ &\leq c\rho_i \sum_{\tau \in \mathcal{T}_h(\partial\Omega_i)} h_\tau^{-2} \|u_i^S\|_{L^2(\tau)}^2 \\ &\leq c\rho_i \sum_{x \in \partial\Omega_{ih}^{CR} \cup \nu_{ih}^{CR}} w_i^2(x) \end{aligned} \tag{37}$$

$$\begin{aligned} &\leq c\rho_i \sum_{\tau \in \mathcal{T}_h(\partial\Omega_i)} h_\tau^{-2} \|u_i - u^0\|_{L^2(\tau)}^2 \\ &\leq c\rho_i h_i^{-2} \sum_{\tau \in \mathcal{T}_h(\partial\Omega_i)} \left\{ \|u_i - \mathcal{M}_i u_i\|_{L^2(\tau)}^2 \right. \\ &\quad \left. + \|\mathcal{M}_i u_i - \alpha_i\|_{L^2(\tau)}^2 \right. \\ &\quad \left. + \|\alpha_i - u^0\|_{L^2(\tau)}^2 \right\} \\ &= c\rho_i h_i^{-2} \{I_1 + I_2 + I_3\}. \end{aligned} \tag{38}$$

It follows immediately from Lemma 1 that I_1 can be estimated as follows

$$\begin{aligned} I_1 &:= \sum_{\tau \in \mathcal{T}_h(\partial\Omega_i)} \|u_i - \mathcal{M}_i u_i\|_{L^2(\tau)}^2 \leq \|u_i - \mathcal{M}_i u_i\|_{L^2(\Omega_i)}^2 \\ &\leq ch_i^2 |u_i|_{h,1(\Omega_i)}^2. \end{aligned}$$

Using Lemma 6 of Chapter 5 in [33], the Poincaré inequality, and Lemma 1 for I_2 , we obtain

$$\begin{aligned} I_2 &:= \sum_{\tau \in \mathcal{T}_h(\partial\Omega_i)} \|\mathcal{M}_i u_i - \alpha_i\|_{L^2(\tau)}^2 \leq cH_i h_i |\mathcal{M}_i u_i|_{H^1(\Omega_i)}^2 \\ &\leq cH_i h_i |u_i|_{h,1(\Omega_i)}^2. \end{aligned}$$

As far as I_3 is concerned, we note that $u^0(x) = \alpha_i$, $x \in \Omega_{ih}^{CR} \setminus \nu_{ih}^{CR}$, and hence

$$I_3 := \sum_{\tau \in \mathcal{T}_h(\partial\Omega_i)} \|\alpha_i - u_i^0\|_{L^2(\tau)}^2 = \|\alpha_i - u_i^0\|_{L^2(\Omega_i)}^2.$$

Now replacing the estimates in (38), adding over $i = 1, \dots, N$, and finally using Lemma 2 for I_3 , we obtain

$$b^S(u^S, u^S) \leq c \frac{H}{h} a(u, u). \tag{39}$$

Taking advantage of Lemma 2, it follows immediately that

$$b^0(u^0, u^0) \leq c \frac{H}{h} a(u, u). \tag{40}$$

Finally,

$$\begin{aligned} \sum_{i=1}^N b^i(u^i, u^i) &= \sum_{i=1}^N a_i(u_i^i, u_i^i) \\ &\leq c \sum_{i=1}^N \left\{ a_i(u, u) + a_i(u_i^0, u_i^0) + a_i(u_i^S, u_i^S) \right\} \\ &= c \left\{ a(u, u) + b^0(u^0, u^0) + b^S(u^S, u^S) \right\} \\ &\leq c \frac{H}{h} a(u, u). \end{aligned} \tag{41}$$

The inequality (35) is a consequence of (39), (40) and (41).

Assumption 2 *The subspaces $V^i, 1 \leq i \leq N$, have no common support. Hence, $\rho(\mathcal{E}) = 1$, where $\rho(\mathcal{E})$ is the spectral radius of $\mathcal{E} = (\delta_{ij})_{1 \leq i, j \leq N}$.*

Assumption 3 *For the subproblems on V^i , where $i \in \{S, 0, \dots, N\}$, exact solvers are used, cf. (11), hence $\omega = 1$.*

4 A more parallel variant of the additive Schwarz method

In this section we split the space V^S one step further in order to get an algorithm which will have much better parallel properties. For the sake of simplicity we assume that the sets $\{v_{mh}\}$ are disjoint. This can be ensured, for instance, by avoiding the case where two mortars meet at a cross point shared by at most two triangles (cf. Fig. 4(left)), or by having at least three triangles in a subdomain, to share a cross point (cf. Fig. 4(right)). The result of the analysis presented in this section applies to the non-disjoint case as well.

Accordingly, we decompose the space V_S into smaller subspaces V^{γ_m} associated with the mortars $\gamma_m \subset S$, by means of

$$V^S = \sum_{\gamma_m \subset S} V^{\gamma_m},$$

where V^{γ_m} is the subspace of V^S , defined as the following.

$$V^{\gamma_m} = \left\{ v \in V^S : v(x) = 0, x \in S_h^{CR} \setminus \{\gamma_{mh}^{CR} \cup v_{mh}^{CR}\} \right\}.$$

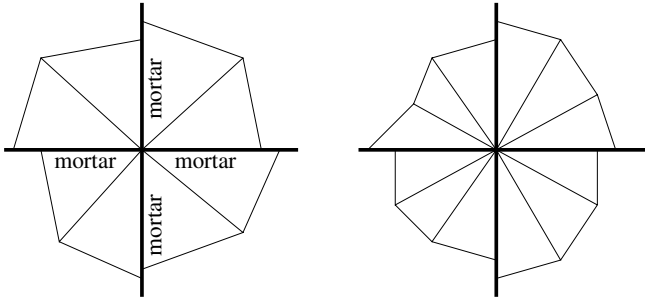


Fig. 4 On the left, two mortar sides meeting at a cross point shared by two triangles in the southeast subdomain, which results into nondisjoint sets $\{v_{mh}\}$. On the right, the number of elements sharing a cross point in each subdomain is three, giving disjoint sets $\{v_{mh}\}$ for any combination of mortar sides

The functions in this space are determined by their values at $\gamma_{mh}^{CR} \cup v_{mh}^{CR}$. Note that the splitting: $V_h = \sum_{\gamma_m \subset \mathcal{S}} V^{\gamma_m} + V^0 + \sum_{i=1}^N V^i$ remains valid. As in the previous method, we use exact bilinear forms for all our subproblems. The operator T in (14), then takes the form: $T = \sum_{\gamma_m \subset \mathcal{S}} T^{\gamma_m} + T^0 + \sum_{i=1}^N T^i$.

Theorem 2 *There exist positive constants c_0 and c_1 , independent of the mesh sizes $h = \inf_i h_i$ and $H = \max_i H_i$, and of the jumps of the coefficients ρ_i , such that for all $u \in V_h$*

$$c_0 \frac{h}{H} a_h(u, u) \leq a_h(Tu, u) \leq c_1 a_h(u, u) . \tag{42}$$

The proof is similar to that of the previous theorem, and so we sketch only the differences here. For Assumption 1, we use the splitting: $u = \sum_{\gamma_m \subset \mathcal{S}} u^{\gamma_m} + \sum_{i=0}^N u^i$, where $u^i, i = 0, \dots, N$ are the same as before. So it remains only to define u^{γ_m} . $u^{\gamma_m} = \{u_i^{\gamma_m}\}_{i=1}^N \in V^{\gamma_m}$ is defined by their nodal values as follows. We note that γ_m is either $\gamma_{m(i)}$ or $\gamma_{m(j)}$ here. If $\gamma_m = \gamma_{m(i)} \subset \partial\Omega_i$, then

$$u_i^{\gamma_{m(i)}}(x) = \begin{cases} w_i(x), & x \in \gamma_{m(i)h}^{CR} \cup v_{m(i)h}^{CR} , \\ 0, & x \in \overline{\Omega}_{ih}^{CR} \setminus \{\gamma_{m(i)h}^{CR} \cup v_{m(i)h}^{CR}\} , \end{cases}$$

and, if $\gamma_m = \gamma_{m(j)} \subset \partial\Omega_j$, where $\gamma_{m(j)} = \delta_{m(i)} \subset \partial\Omega_i$, then

$$u_i^{\gamma_{m(j)}}(x) = \begin{cases} w_i(x), & x \in \delta_{m(i)h}^{CR}, \gamma_{m(j)} = \delta_{m(i)} , \\ 0, & x \in \overline{\Omega}_{ih}^{CR} \setminus \delta_{m(i)h}^{CR} , \end{cases}$$

It is not difficult to see that $u = \sum_{\gamma_m \subset \mathcal{S}} u^{\gamma_m} + \sum_{i=0}^N u^i$. For $u^{\gamma_m} = \{u_i^{\gamma_m}\}_{i=1}^N \in V^{\gamma_m}$, we have

$$\sum_{\gamma_m \subset \mathcal{S}} b^{\gamma_m}(u^{\gamma_m}, u^{\gamma_m}) = \sum_{i=1}^N \sum_{\gamma_m \subset \mathcal{S}} a_i(u_i^{\gamma_m}, u_i^{\gamma_m}) .$$

By the inverse inequality, we obtain

$$\begin{aligned}
 \sum_{\gamma_m \subset \mathcal{S}} a_i(u_i^{\gamma_m}, u_i^{\gamma_m}) &= \sum_{\gamma_m \subset \mathcal{S}} \rho_i \sum_{\tau \in \mathcal{T}_h(\Omega_i)} |u_i^{\gamma_m}|_{H^1(\tau)}^2 \\
 &\leq c \sum_{\gamma_m \subset \mathcal{S}} \rho_i \sum_{\tau \in \mathcal{T}_h(\partial\Omega_i)} h_\tau^{-2} \|u_i^{\gamma_m}\|_{L^2(\tau)}^2 \\
 &\leq c\rho_i \sum_{x \in \partial\Omega_{ih}^{CR} \cup v_{ih}^{CR}} w_i^2(x),
 \end{aligned}$$

an expression which is the same as in (37). The proof of Assumption 1 thus follows from before. For Assumption 2, we treat only V^0 as the coarse problem. Though the subspaces $V^i, i = 1, \dots, N$, do not have common support with each other, they do have with the subspaces V^{γ_m} . The later may even have common support with each other. Using the strengthened Cauchy Schwarz inequality, one can bound ρ by a constant which depends on the maximum number of subdomains sharing a cross point. The proof of the theorem then follows.

5 Numerical results

In this section, we show the performance of our additive Schwarz methods for the lowest order Crouzeix-Raviart mortar finite element, introduced in this paper. For the experiments, we define our model problem to be defined on a unit square domain, and consider the domain to be the union of 2×2 nonoverlapping square subregions, each with a coefficient ρ_i (the material property) chosen from $\{\rho, 1\}$ in a checkerboard order (cf. Figure 5). So, ρ defines the size of the jumps in the coefficients. We refer to an interface between two such subregions as a material interface. The forcing function f is chosen such that the exact solution u is equal to $\sin(\pi x) \sin(\pi y)$. Note that $\nabla u \cdot \eta$ vanishes along the subregion interfaces.

The numerical solution to this problem is then found either by solving the original system (4) using the Conjugate Gradients (CG) method, or by solving the

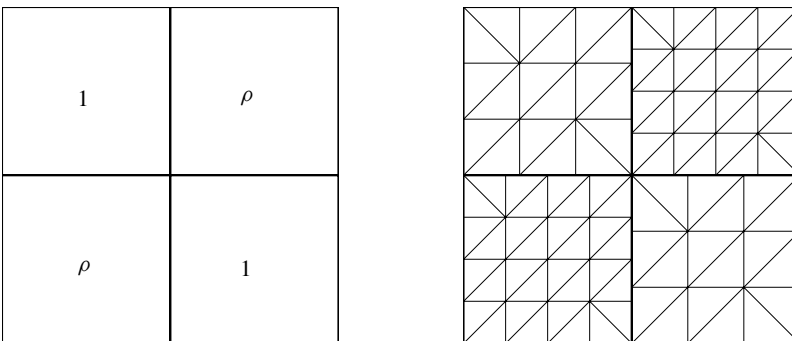


Fig. 5 Distribution of coefficients in the model problem (left), and an example of a nonmatching discretization of the 2×2 subdomains (right)

equivalent preconditioned system (14) using the Preconditioned Conjugate Gradients method (PCG). Note that both systems result in symmetric and positive definite operators. The CG (PCG) iteration stops whenever the residual norm is reduced by the factor 10^{-6} . An estimate for the condition number of the corresponding system is calculated using the Lanczos connection to the CG iteration [25].

The discretization is done as follows: Initially, for some nonzero d the domain is partitioned into $d \times d$ nonoverlapping rectangular subdomains. For the model problem, d is always chosen as an integer multiple of 2 so that no material interface can cut a subdomain. Each subdomain is then discretized uniformly using, in a checkerboard order, either $2n^2$ or $2(n - 1)^2$ right angle triangles of the same size, for some $n > 1$. Note that every two neighboring subdomains get nonmatching grids across their interface. See Figure 5 for an illustration.

An overlapping Schwarz method with minimal overlap We note that the methods proposed in this paper are of nonoverlapping nature, i.e., nonoverlapping in the sense that the subproblems associated with the subdomains can be solved independently, and for the other subproblems we can have their copies in as many processors (virtual processors) as necessary in order to avoid exchange of information between processors. For the sake of comparison, we introduce, without the convergence analysis, a new overlapping variant of the additive Schwarz method with minimal overlap and a coarse space. Numerical experiments have shown that its convergence behavior is similar to that of the standard overlapping Schwarz method with a coarse space for conforming elements. We split V_h as $V_h = V^0 + \sum_{i=1}^N \hat{V}^i$, where the subspace \hat{V}^i , associated with the subdomain Ω_i , is chosen as $\hat{V}^i = V^i + \sum_{\gamma_{m(i)} \subset S} V^{\gamma_{m(i)}}$, where the sum is taken over the mortars, $\gamma_{m(i)}$, those belonging to Ω_i only. The coarse space V^0 is the same as in the proposed methods, and the subproblem solvers are the exact solvers.

In our first experiment (cf. Table 1), we compare the three variants of the additive Schwarz method, the overlapping variant (“Overlapping_y”), and the proposed variants, the original (“Proposed_{orig}”) and the modified (“Proposed_{mod}”), showing condition number estimates for the preconditioned systems, the number of PCG iterations (in parentheses) for a fixed $\frac{H}{h}$ ratio. This ratio has been kept fixed by fixing the number of triangles in each subdomain which, in this experiment, equals to either 72 or 50 ($n = 6$). In order to have disjoint sets $\{v_{mh}\}$, we choose the north- and the south sides or the east- and west sides of a subdomain as the mortar sides. As seen from the table, for the fixed $\frac{H}{h}$ ratio, the condition number

Table 1 Condition number estimates, PCG-iteration counts (in parentheses) for a fixed $\frac{H}{h}$ ratio and the jump size $\rho = 10^4$

Subdomains $d \times d$	Additive Schwarz method		
	Overlapping _y	Proposed _{orig}	Proposed _{mod}
6×6	30.32 (39)	35.22 (44)	38.14 (46)
8×8	30.96 (42)	35.57 (47)	38.03 (47)
12×12	32.03 (44)	36.33 (48)	37.92 (50)

Table 2 Condition number estimates and PCG-iteration counts (in parentheses) for different values of jumps in the coefficients.

	Checkerboard distribution of coefficients $\{\rho, 1\}$			
	$\{10^0, 1\}$	$\{10^2, 1\}$	$\{10^4, 1\}$	$\{10^6, 1\}$
PCG	31.01 (34)	31.61 (34)	31.64 (31)	31.64 (31)
CG	$9.03 \cdot 10^2$ (91)	$2.28 \cdot 10^4$ (469)	$2.25 \cdot 10^6$ (1099)	$2.24 \cdot 10^8$ (1250)

estimates and consequently the number of iterations remain bounded illustrating that the methods are all quasi-optimal (optimal with respect to a fixed $\frac{H}{h}$ ratio). Although the overlapping method has the best estimates, the proposed methods show the corresponding estimates which are comparable to those. As seen from the table, the proposed original method converges slightly faster than the proposed modified method. However, the latter one is expected to be more attractive with respect to their parallel properties. Further experiments have confirmed the linear dependence of the condition number estimate on the above mesh size ratio as the theory predicts.

Finally, we state that the additive Schwarz methods are all robust with respect to coefficient jumps. In the Table 2, we report results for the proposed original method only (cf. the first row “PCG”). Estimates in the table, are given for different values of jumps in the coefficients, varying as 1, 10^2 , 10^4 , and 10^6 . Here, a partition of 4×4 subdomains has been considered, where each subdomain contains either 72 or 50 ($n = 6$) triangles. For comparison, results for the original system are also provided (cf. the second row (“CG”) in the table). As we can see from the table, the condition number estimates - consequently the number of CG iterations - for the original system deteriorate rapidly with the increase in the jumps, whereas those for the preconditioned system remain bounded.

Acknowledgements The authors would like to thank the anonymous referees for their valuable comments and suggestions which have led to a much improved paper.

References

1. Achdou, Y., Maday, Y., Widlund, O.B.: Iterative substructuring preconditioners for mortar element methods in two dimensions. *SIAM J. Numer. Anal.* **36**, 551–580 (1999)
2. Arbogast, T., Chen, Z.: On the implementation of mixed methods as nonconforming methods for second-order elliptic problems. *Math. Comp.* **64**, 943–972 (1995)
3. Arnold, D.N., Brezzi, F.: Mixed and nonconforming finite element methods: implementation, postprocessing and error estimates. *RAIRO Math. Modelling and Numer. Anal.* **19**, 7–32 (1985)
4. Ben Belgacem, F.: The mortar element method with Lagrange multipliers. Université Paul Sabatier, Toulouse, France, 1994
5. Ben Belgacem, F., Maday, Y.: The mortar element method for three dimensional finite elements. *RAIRO Math. Modelling and Numer. Anal.* **31**, 289–302 (1997)
6. Bernardi, C., Maday, Y., Patera, A.T.: A new non conforming approach to domain decomposition: The mortar element method. In: Collège de France Seminar, H. Brezis, J.-L. Lions (eds.), Pitman, 1994. This paper appeared as a technical report about five years earlier
7. Bernardi, C., Verfürth, R.: Adaptive finite element methods for elliptic equations with non-smooth coefficients. *Numerische Mathematik*, **85**, 579–608 (2000)

8. Bjørstad, P., Dryja, M., Rahman, T.: Additive Schwarz for anisotropic elliptic problems. In: *Parallel Solution of Partial Differential Equations*, P. Bjørstad, M. Luskin (eds.), vol. 120 of IMA Volumes in Mathematics and its Applications, Springer-Verlag New York, 2000, pp. 279–294
9. Bjørstad, P., Dryja, M., Rahman, T.: Additive Schwarz methods for elliptic mortar finite element problems. *Numerische Mathematik* **95**, 427–457 (2003)
10. Bjørstad, P., Dryja, M., Vainikko, E.: Additive Schwarz methods without subdomain overlap and with new coarse spaces. In: *Domain Decomposition Methods in Sciences and Engineering*, R. Glowinski, J. Périaux, Z. Shi, O. B. Widlund (eds.), John Wiley & Sons, 1997. *Proceedings from the Eight International Conference on Domain Decomposition Methods*, May 1995, Beijing
11. Bjørstad, P.E., Dryja, M.: A coarse space formulation with good parallel properties for an additive Schwarz domain decomposition algorithm. Unpublished document 1999, University of Bergen
12. Braess, D., Dahmen, W.: Stability estimates of the mortar finite element method for 3-dimensional problems. *East-West J. Numer. Math.* **6**, 249–264 (1998)
13. Braess, D., Dahmen, W.: The mortar element method revisited – what are the right norms?. In *Thirteenth international conference on domain decomposition*, 2001, pp. 245–252
14. Braess, D., Dryja, M., Hackbusch, W.: A multigrid method for nonconforming fe-discretizations with application to non-matching grids. *Computing* **63**, 1–25 (1999)
15. Brenner, S.C.: Two-level additive Schwarz preconditioners for nonconforming finite element methods. *Math. Comput.* **65**, 897–921 (1996)
16. Casarin, M.A., Widlund, O.B.: A hierarchical preconditioner for the mortar finite element method. *ETNA* **4**, 75–88 (1996)
17. Chen, Z.: Analysis of mixed methods using conforming and nonconforming finite element methods. *RAIRO Math. Modelling and Nume. Anal.* **27**, 9–34 (1993)
18. Ciarlet, P.G.: *The Finite Element Method for Elliptic Problems*. North-Holland, Amsterdam, 1978
19. Cowsar, L.C.: Domain decomposition methods for nonconforming finite elements. Tech. Report TR93-09, Department of Mathematical Sciences, Rice University, March 1993
20. Deng, Q.: A nonoverlapping domain decomposition method for nonconforming finite element problems. *Commun. Pure Appl. Anal.* **2**, 295–306 (2003)
21. Dryja, M.: Additive Schwarz methods for elliptic mortar finite element problems. In: *Modeling and Optimization of Distributed Parameter Systems with Applications to Engineering*, K. Malanowski, Z. Nahorski, M. Peszynska (eds.), IFIP, Chapman & Hall, London, 1996
22. Dryja, M.: An iterative substructuring method for elliptic mortar finite element problems with discontinuous coefficients. In: *The Tenth International Conference on Domain Decomposition Methods*, J. Mandel, C. Farhat, X.-C. Cai (eds.) *Contemporary Mathematics* 218, AMS, 1998, pp. 94–103
23. Dryja, M., Sarkis, M.V., Widlund, O.B.: Multilevel Schwarz methods for elliptic problems with discontinuous coefficients in three dimensions. *Numerische Mathematik* **72**, 313–348 (1996)
24. Dryja, M., Widlund, O.B.: Schwarz methods of Neumann-Neumann type for three-dimensional elliptic finite element problems. *Commun. Pure Appl. Math.* **48**, 121–155 (1995)
25. Golub, G.H., Loan, C.F.V.: *Matrix Computations*. Johns Hopkins Univ. Press, 1989. Second Edition
26. Gopalakrishnan, J., Pasciak, J.E.: Multigrid for the mortar finite element method. *SIAM J. Numer. Anal.* **37**, 1029–1052 (2000)
27. Hoppe, R.H.W., Wohlmuth, B.: Adaptive multilevel iterative techniques for nonconforming finite element discretizations. *East-West J. Numer. Math.* **3**, 179–197 (1995)
28. Lazarov, R.D., Margenov, S.D.: On a two-level parallel MIC(0) preconditioning of Crouzeix-Raviart non-conforming FEM systems. In: *Numerical methods and applications. Proceedings. 5th Int. Conf. NMA2002*, Borovets, Bulgaria, August 20–24, 2002, vol. 2542 of LNCS, Springer-Verlag, 2003, pp. 192–201
29. Marcinkowski, L.: The mortar element method with locally nonconforming elements. *BIT* **39**, 716–739 (1999)
30. Sarkis, M.: Two-level Schwarz methods for nonconforming finite elements and discontinuous coefficients. In: *Proceedings of the Sixth Copper Mountain Conference on Multigrid Methods*, Volume 2, N.D. Melson, T.A. Manteuffel, S.F. McCormick (eds.), no. CP 3224, Hampton VA, 1993, NASA, pp. 543–566

31. Sarkis, M.: Nonstandard coarse spaces and Schwarz methods for elliptic problems with discontinuous coefficients using non-conforming element. *Numerische Mathematik* **77**, 383–406 (1997)
32. Seshaiyer, P., Suri, M.: Uniform hp convergence results for the mortar finite element method. *Math. Comput.* **69**, 521–546 (1999)
33. Smith, B., Bjørstad, P., Gropp, W.: *Domain Decomposition: Parallel Multilevel Methods for Elliptic Partial Differential Equations*. Cambridge University Press, 1996
34. Wieners, C., Wohlmuth, B.: The coupling of mixed and conforming finite element discretizations. In: *Domain Decomposition Methods 10*, J. Mandel, C. Farhat, X.C. Cai, (eds.), AMS, 1998, pp. 453–459. Proceedings from the Tenth International Conference, June 1997, Boulder, Colorado
35. Wohlmuth, B.: Mortar finite element methods for discontinuous coefficients. *ZAMM* **79**(S I), 151–154 (1999)
36. Wohlmuth, B.: A residual based error estimator for mortar finite element discretizations. *Numerische Mathematik* **84**, 143–171 (1999)
37. Wohlmuth, B.: A mortar finite element method using dual spaces for the Lagrange multiplier. *SIAM J. Numer. Anal.* **38**, 989–1012 (2000)
38. Wohlmuth, B., Hoppe, R.H.W.: Multilevel approaches to nonconforming finite element discretizations of linear second order elliptic boundary value problem. *J. Comput. Information* **4**, 73–86 (1994)
39. Xu, J., Zou, J.: Some nonoverlapping domain decomposition methods. *SIAM Review* **40**, 857–914 (1998)
40. Xu, X., Chen, J.: Multigrid for the mortar element method for p1 nonconforming element. *Numerische Mathematik* **88**, 381–398 (2001)
41. Yang, D.: Finite elements for elliptic problems with wild coefficients. *Mathematics and Computers in Simulation* **54**, 383–395 (2000)